HHS Public Access

Author manuscript

J Am Chem Soc. Author manuscript; available in PMC 2021 July 01.

Published in final edited form as:

J Am Chem Soc. 2020 July 01; 142(26): 11388–11393. doi:10.1021/jacs.0c05362.

Site-Selective Copper-Catalyzed Azidation of Benzylic C—H Bonds

Sung-Eun Suh[†], **Si-Jie Chen**[†], **Mukunda Mandal**[‡], **Ilia A. Guzei**[†], **Christopher J. Cramer**[‡], **Shannon S. Stahl**[*,†]

[†]Department of Chemistry, University of Wisconsin–Madison, 1101 University Avenue, Madison, Wisconsin 53706, United States

[‡]Department of Chemistry, Chemical Theory Center and Supercomputing Institute, University of Minnesota, Minneapolis, Minnesota 55455, United States

Abstract

Site selectivity represents a key challenge for nondirected C—H functionalization, even when the C—H bond is intrinsically reactive. Here, we report a copper-catalyzed method for benzylic C—H azidation of diverse molecules. Experimental and density functional theory studies suggest the benzyl radical reacts with a Cu^{II}-azide species via a radical-polar crossover pathway. Comparison of this method with other C—H azidation methods highlights the unique site-selectivity of this method, and conversions of the benzyl azide products into amine, triazole, tetrazole, and pyrrole functional groups highlight the broad utility of this method for target molecule synthesis and medicinal chemistry.

Graphical Abstract

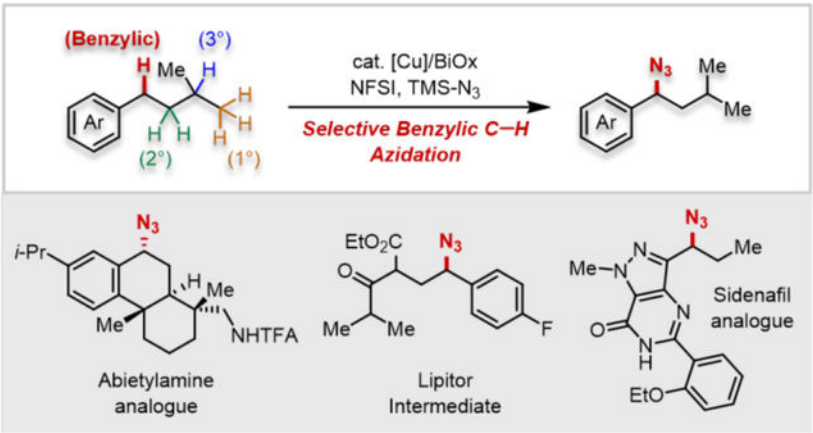

[*]**Corresponding Author** stahl@chem.wisc.edu.

Supporting Information.

The Supporting Information is available free of charge on the ACS Publications website at DOI: https://doi.org/10.1021/jacs.0c05362 Experimental details with screening results, characterization data, and NMR spectra (PDF), X-ray crystal structure data for $[(BPhen)Cu^{II}(N_3)(\mu\text{-}N_3)]_2$ (CIF), and DFT computational results, including xyz coordinates for computed structures.

The authors declare no competing financial interest.

C—H functionalization methods improve the efficiency of target molecule syntheses[1-3] and expand the scope of accessible structures.[4] The large number of C—H bonds within individual molecules, however, introduces site-selectivity challenges.[1,5,6] Organic azides are versatile synthetic intermediates.[7-9] They represent effective ammonia surrogates,[10] are readily converted into *N*-heterocycles, [11, 12] and provide access to important bioactive molecules. (Figures 1A and 1B).[13-15] Recent efforts have demonstrated C(sp^3)—H azidation,[16] including iron-[17,18] and manganese-catalyzed[19] and photochemical[20,21] methods that are compatible with diverse C—H substrates as the limiting reagent. These methods proceed via radical intermediates that show high selectivity for tertiary over primary and secondary aliphatic C—H bonds, but selectivity for benzylic over aliphatic positions is relatively low[20] or has not been investigated. Benzylic and heterobenzylic C—H bonds are ubiquitous in bioactive molecules, and site-selective functionalization of such positions could have broad impact. We [22, 23] and others [24-27] have reported copper catalysts with *N*-fluorobenzenesulfonimide (NFSI) that enable selective functionalization of benzylic C—H bonds.[28-30] Here, we describe a similar approach for C—H azidation that exhibits unique benzylic site-selectivity relative to other azidation methods (Figure 1C). Complementary studies provide mechanistic insights into the reaction and showcase the synthetic utility in the preparation of important target molecules.

Initial reaction optimization efforts used 1-ethylnaphthalene **3a** and $TMSN_3$ as coupling partners. An initial attempt with previous benzylic C—H cyanation conditions[22] led to the desired product, but with low conversion and yield (6%, entry1, Table 1). Increasing the temperature to 50 °C and using nitromethane as the solvent significantly increased the yield of **4a** (entries 2 and 3, Table 1; see Tables S1-S9 in the Supporting Information for full screening data). Cu^I and Cu^{II} acetate salts were the most effective catalyst precursors (entries 3 and 6). $Cu(OAc)_2$ was selected because it led to higher yields, and its air-stability facilitated handing. Testing the reaction without **L1** highlighted the importance of an ancillary ligand (entry 7). Screening other ligands (entries 8-10 and Table S4) showed that improved yields could be obtained with 2,2'-bioxazoline (BiOx) ligands (e.g., 85% yield with **L4**, entry 10). Further screening led to the optimized conditions in entry 11, affording 93% yield of azide **4a**. The lack of enantioselectivity, even with a single enantiomer of the ligand, prompted several efforts to probe the reaction mechanism.

Cu^I-mediated reductive activation of NFSI will generate an imidyl radical that promotes hydrogen-atom transfer (HAT) from the benzylic C—H bond.[23] The resulting benzyl radical can react with a Cu^{II}-azide species to afford the benzyl azide. Under simulated catalytic conditions lacking the benzylic substrate, Cu^IOAc, **L2**, NFSI, and $TMSN_3$ generate a dimeric Cu^{II}-azide complex, characterized by X-ray crystallography (Figure 2A). Addition of Gomberg's dimer,[31] which readily dissociates into two trityl radicals, to a solution of this complex generated trityl azide in 91% yield (Figure 2B).[32,33] This stoichiometric reaction was complemented by a catalytic reaction with triphenylmethane, which afforded the benzyl azide in 66% yield.

Seminal studies by Kochi suggest several possible pathways for C—N bond formation (Figure 3A).[34-39] In Path I, the benzyl radical adds to Cu^{II} to generate a benzyl-Cu^{III} species that can undergo C—N reductive elimination.[22,34] Path II includes multiple pathways

involving radical attack at a terminal or bridging azide ligand, either at the proximal or distal *N*-atom of the azide.[35-37] Finally, Path III involves one-electron oxidation of the benzyl radical by Cu^{II} to generate a cation, which can react readily with an azide nucleophile.[23,38,39] Density functional theory calculations were performed to assess relevant structures and the energies of these pathways (M06-L/basis-II/SMD($MeNO_2$); B3LYP-D3(BJ)/basis-I level of theory: Basis-I = 6–31G(d,p) for non-metals; SDD basis and pseudopotential for Cu. Basis-II = def2-TZVP for non-metals, def2-TZVP basis and SDD pseudopotential for Cu; see Section 9 in Supporting Information). The energy diagrams in Figure 3B highlight the most favorable energies identified for Paths I–III involving reaction of the benzyl radical of 1-ethylnaphthalene and **L4**-ligated Cu^{II}-dimer. The results show that radical addition to Cu^{II}, followed by C—N reductive elimination from **Int-1** has the highest energy among the different mechanisms (Figure 3B). Radical addition to an azide ligand proceeds with much lower barrier. The pro-*R* face favors addition to a bridging azide while the pro-*S* favors addition to a terminal azide: $\Delta G^{\ddagger}$ = 2.6 and 2.4 kcal/mol for ^{R}**TS2** and ^{S}**TS2**, respectively. In both cases, radical addition is favored at the distal *N*-atom of the azide ligand. Computational analysis of the electron-transfer pathway leveraged the experimental redox potential measured for $[(BPhen)Cu^{II}(N_3)(\mu\text{-}N_3)]_2$ (−0.16 V vs. $Fc^{0/+}$; see Figure S8) and reported potentials for the benzyl radicals of ethylbenzene and isopropylbenzene ($E^{\circ}_{R^+|R^{\bullet}}$ = −0.01 and −0.22 V vs. $Fc^{0/+}$).[40] Using these values as benchmarks, calculated redox potentials for $[(\mathbf{L4})Cu^{II}(N_3)(\mu\text{-}N_3)]_2$ and the benzyl radical of **3a** reveal that oxidation of the radical by the Cu^{II}-dimer is thermodynamically favorable (ΔG° = −0.8 kcal/mol). The small calculated energy difference between Paths II and III, and the absence of an electron-transfer rate constant, prevent clear distinction between these two paths on the basis of computational studies; however, both are predicted to afford little or no enantioselectivity.[41] Experimental data providing some support for Path III was obtained from catalytic azidation of 4-Ph-cumene. Benzylic azidation was observed in 2:1 ratio with a vicinal diazide byproduct. Control experiments suggest diazidation arises from an α-methylstyrene intermediate (see Figures S3 and S4). These results are most consistent with a radical-polar crossover mechanism, in which the benzyl cation is trapped by an azide nucleophile or loses a proton to generate an alkene, which can undergo subsequent 1,2-diazidation.

Efforts were then made to explore the site-selectivity of this method (Figure 4). Three substrates incorporating both secondary benzylic and tertiary aliphatic C—H bonds were selected: isobutylbenzene **3b**, isopentylbenzene **3c**, and ibuprofen methyl ester **3d**. Use of the Cu/NFSI catalytic conditions at 30 °C led to azidation yields of 48%, 71%, and 62%, respectively, with benzylic:tertiary (B:T) selectivity ranging from 11:1–30:1. No azidation was observed at the tertiary benzylic position adjacent to the ester in **3d**. This result probably reflects both steric inhibition and a polarity mismatch in reaction with the sulfonimidyl radical. These results were compared to analogous data from three other C—H azidation methods, including photochemical,[20] Mn-catalyzed,[19] and Fe-catalyzed[17-18] reactions (II–IV, Figure 4). The reported site-selectivity for **3b** and **3d** with method II exhibit a B:T ratio of ~ 1:1.[20] Independent testing of **3c** revealed tertiary C—H azidation. Mn(salen)Cl with PhIO (method III)[19] also exhibits good selectivity for benzylic azidation: B:T = 4.6:1, 4.6:1, and 14:1, respectively, for **3b**, **3c**, and **3d**, although these reactions were operationally more challenging and led to lower yields (28–48%) than Cu/NFSI. The $Fe(OAc)_2/I^{III}$-azide system

(method IV)[17-18] showed relatively low B:T selectivity with **3b**–**3d** (1:1–2.5:1). Collectively, the data in Figure 4 show that Cu/NFSI exhibits unique benzylic site-selectivity.

Expanding on the results obtained with substrates **3a**–**3d**, we evaluated the azidation of other benzylic C—H substrates (Table 2). Reactions of various *para*-substituted ethylbenzenes (4-Ph, -Br, -OAc, and -OMe) resulted in moderate-to-good yields (45-81%, **4e**–**4h**). An exception was the electron-deficient 4-CN derivative **4j** (25%), while an aliphatic nitrile was better tolerated (**4k**, 51%). The common pharmacophore chroman[42] underwent azidation in 60% yield (**4l**), and tetralin and benzosuberan, containing 6- and 7-membered rings, afforded good yields of **4m** (90%) or **4n** (85%). In contrast, indane led to only 12% yield of the azide, together with various byproducts (see Table S13 for a summary of this and other unsuccessful substrates). Bibenzyl underwent selective mono-azidation (72%, **4o**), and a series of diarylmethane derivatives, which are common pharmaceutical core structures, accessed moderate-to-good azide product yields (**4p**–**4s**).[43] Substrate **3t** underwent azidation at two sites: adjacent to the carbonyls of the ketoester and at the benzylic position (**4t**/**4u**). Increasing the temperature to 60 °C led to exclusive azidation at the α-C—H bond of the ketoester. Heterobenzylic substrates with pyridine and pyrazole units afforded the desired azides **4v**–**4x** in moderate yield (30-65%), demonstrating tolerance to pharmaceutically relevant heterocycles.

The azidation reaction was also used in late-stage functionalization of drug molecules and derivatives. Examples include azidation of precursors to sildenafil[44] with a nitrogen heterocycle (**4y**); dronedarone [45] with a benzofuran (**4z**); canagliflozin[46] with a thiophene (**4aa**), and the natural product desoxyanisoin (**4ab**). [47] The tetrahydroquinoline of a GnRH antagonist[48] precursor led to reaction at the benzylic position (**4ac**), with no byproduct observed from reaction adjacent to nitrogen. The tetraacetate derivative of dapagliflozin [49] reacted at the benzhydryl position, rather than the benzyl ether (**4ad**). Dehydroabietylamine derivative **3ae** features three potential sites for functionalization, a tertiary aliphatic and secondary and tertiary benzylic C—H bonds. Only the secondary benzyl azide (−)-**4ae** was observed (62% yield, 0.5 g). Finally, azidation of celestolide[50] proceeded in excellent yield to **4af** (92%, 1.25 g).

The appeal of the benzylic C—H azidation reactions in Table 2 is amplified by opportunities for further elaboration of the azide unit. For example, azides are highly effective ammonia surrogates. A Staudinger reduction of the azide in (−)-**4ae** proceeded efficiently to (−)-**5** in 91% yield with a phosphine resin that facilitates product isolation (Figure 5A). This route to (−)-**5** is an appealing alternative to a recently reported route involving Mn-catalyzed C—H amidation of **3ae** with a sulfamate ester, followed by reductive deprotection of the sulfamate to afford (−)-**5** in 43% overall yield.[29] Azides are also versatile precursors to pharmaceutically important heterocycles. The formal synthesis of Lipitor, **2**, a lipid-lowering drug,[51] was achieved via conversion of azido compound **4t** into the pyrrole precursor to Lipitor (**6**, Figure 5B; cf. Figure 1).[14,15] The anti-tuberculosis agent **7**, used against mycobacterium tuberculosis strain $H_{37}RV$, was synthesized via copper-catalyzed alkyne-azide cycloaddition of **4n** with *m*-methoxyphenylacetylene (Figure 5C).[52] The related [3+2]-

cycloaddition of **4af** with ethyl cyanoformate gave two regioisomeric celestolide analogues (**8** and **9**) in quantitative yield (Figure 5D).

The results described herein demonstrate that a copper-based catalyst system composed entirely of commercially available components enables selective benzylic C—H azidation with broad scope. The reaction is initiated by hydrogen-atom transfer, followed by reaction of the benzylic radical with a Cu^{II}-azide intermediate. Experimental and computational data support a radical-polar crossover pathway involving a benzylic cation. The unique combination of good yields, diverse functional group compatibility, and high benzylic site-selectivity make this method well-suited for the incorporation of primary amines and azide-derived heterocycles (pyrroles, triazoles, and tetrazoles) into pharmaceutical and agrochemical building blocks, intermediates, and existing bioactive molecules.

Supplementary Material

Refer to Web version on PubMed Central for supplementary material.

ACKNOWLEDGMENT

This work was supported by funding from the NIH (R01 GM126832 and R35 GM134929). Spectroscopic instrumentation was supported by a gift from Paul. J. Bender, the NSF (CHE-1048642), and the NIH (1S10 OD020022-1). Mukunda Mandal acknowledges a doctoral dissertation fellowship from the University of Minnesota. The authors thank Dr. Joshua A. Buss for providing a sample of Gomberg's dimer and Amelia M. Wheaton for X-ray crystallographic assistance.

REFERENCES

1. Hartwig JF Catalyst-Controlled Site-Selective Bond Activation. Acc. Chem. Res 2017, 50, 549–555. [PubMed: 28945414]
2. Stang EM; White MC Total Synthesis and Study of 6-Deoxyerythronolide B by Late-Stage C—H Oxidation. Nat. Chem 2009, 1, 547–551. [PubMed: 21378935]
3. Rosen BR; Simke LR; Thuy-Boun PS; Dixon DD; Yu J-Q; Baran PS C—H Functionalization Logic Enables Synthesis of (+)-Hongoquercin A and Related Compounds Angew. Chem., Int. Ed 2013, 52, 7317–7320.
4. Cernak T; Dykstra KD; Tyagarajan S; Vachal P; Krska SW The Medicinal Chemist's Toolbox for Late Stage Functionalization of Drug-Like Molecules. Chem. Soc. Rev 2016, 45, 546–576. [PubMed: 26507237]
5. Newhouse T; Baran PS If C—H Bonds Could Talk: Selective C—H Bond Oxidation. Angew. Chem., Int. Ed 2011, 50, 3362–3374.
6. Hartwig JF; Larsen MA Undirected, Homogeneous C—H Bond Functionalization: Challenges and Opportunities. ACS Cent. Sci 2016, 2, 281–292. [PubMed: 27294201]
7. Wang X; Huang B; Liu X; Zhan P Discovery of Bioactive Molecules from CuAAC Click-Chemistry-Based Combinatorial Libraries. Drug Discov. Today 2016, 21, 118–132. [PubMed: 26315392]
8. El-Sagheer AH; Brown T Click Nucleic Acid Ligation: Applications in Biology and Nanotechnology. Acc. Chem. Res 2012, 45, 1258–1267. [PubMed: 22439702]
9. Pickens CJ; Johnson SN; Pressnall MM; Leon MA; Berkland CJ Practical Considerations, Challenges, and Limitations of Bioconjugation via Azide–Alkyne Cycloaddition. Bioconjugate Chem. 2018, 29, 686–701.
10. Gololobov YG; Kasukhin LF Recent Advances in the Staudinger Reaction. Tetrahedron 1992, 48, 1353–1406.

11. Bräse S; Gil C; Knepper K; Zimmermann V Organic Azides: An Exploding Diversity of a Unique Class of Compounds. Angew. Chem. Int. Ed 2005, 44, 5188–5240.
12. Padwa A Aziridines and Azirines: Monocyclic In Comprehensive Heterocyclic Chemistry III; Katritzky AR; Ramsden CA; Scriven EFV; Taylor RJK, Eds.; Elsevier Science: Oxford, 2008; Vol. 1, Chapter 1.01.6.2, pp 50–64.
13. Li Y-L; Combs AP; Bicyclic Heteroarylaminoalkyl Phenyl Derivatives as PI3K Inhibitors, International Patent 2015191677A1, 12 17, 2015.
14. Ivanov KL; Villemson EV; Budynina EM; Ivanova OA; Trushkov IV; Melnikov MY Ring Opening of Donor-Acceptor Cyclopropanes with the Azide Ion: A Tool for Construction of N-Heterocycles. Chem. Eur. J 2015, 21, 4975–4987. [PubMed: 25573783]
15. Kim M-S; Yoo M-H; Rhee J-K; Kim Y-J; Park S-J; Choi J-H; Sung S-Y; Lim H-G; Cha D-W; Synthetic Intermediates, Process for Preparing Pyrrolylheptanoic Acid Derivatives Therefrom. International Patent 2009084827A3, 7 9, 2009.
16. Goswami M; de Bruin B Metal-Catalysed Azidation of Organic Molecules. Eur. J. Org. Chem 2017, 2017, 1152–1176.
17. Karimov RR; Sharma A; Hartwig JF Late Stage Azidation of Complex Molecules. ACS Cent. Sci 2016, 2, 715–724. [PubMed: 27800554]
18. Sharma A; Hartwig JF Metal-Catalysed Azidation of Tertiary C—H Bonds Suitable for Late-Stage Functionalization. Nature 2015, 517, 600–604. [PubMed: 25631448]
19. Huang X; Bergsten TM; Groves JT Manganese-Catalyzed Late-Stage Aliphatic C—H Azidation. J. Am. Chem. Soc 2015, 137, 5300–5303. [PubMed: 25871027]
20. Margrey KA; Czaplyski WL; Nicewicz DA; Alexanian EJ A General Strategy for Aliphatic C—H Functionalization Enabled by Organic Photoredox Catalysis. J. Am. Chem. Soc 2018, 140, 4213–4217. [PubMed: 29522330]
21. Wang Y; Li G-X; Yang G; He G; Chen G A Visible-Light-Promoted Radical Reaction System for Azidation and Halogenation of Tertiary Aliphatic C—H Bonds. Chem. Sci 2016, 7, 2679–2683. [PubMed: 28660040]
22. Zhang W; Wang F; McCann SD; Wang D; Chen P; Stahl SS; Liu G Enantioselective Cyanation of Benzylic C—H Bonds via Copper-Catalyzed Radical Relay. Science 2016, 353, 1014–1018. [PubMed: 27701109]
23. Hu H; Chen S-J; Mandal M; Pratik SM; Buss JA; Krska SW; Cramer CJ; Stahl SS Copper-Catalyzed Benzylic C—H Coupling with Alcohols via Radical Relay Enabled by Redox Buffering. Nat. Catal 2020, 3, 358–367. [PubMed: 32368720]
24. Ni Z; Zhang Q; Xiong T; Zheng Y; Li Y; Zhang H; Zhang J; Liu Q Highly Regioselective Copper-Catalyzed Benzylic C—H Amination by *N*-Fluorobenzenesulfonimide Angew. Chem., Int. Ed 2012, 51, 1244–1247.
25. Zhang W; Chen P; Liu G Copper-Catalyzed Arylation of Benzylic C—H Bonds with Alkylarenes as the Limiting Reagents. J. Am. Chem. Soc 2017, 139, 7709–7712. [PubMed: 28562032]
26. Zhang W; Wu L; Chen P; Liu G Enantioselective Arylation of Benzylic C—H Bonds by Copper-Catalyzed Radical Relay. Angew. Chem. Int. Ed 2019, 58, 6425–6429.
27. Xiao H; Liu Z; Shen H; Zhang B; Zhu L; Li C Copper-Catalyzed Late-Stage Benzylic C(sp^3)—H Trifluoromethylation. Chem 2019, 5, 940–949.
28. Complementary C—H functionalization methods showing high benzylic site selectivity have been reported recently. See refs. 29 and 30.
29. Clark JR; Feng K; Sookezian A; White MC Manganese-Catalysed Benzylic C(sp^3)—H Amination for Late-Stage Functionalization. Nat. Chem 2018, 10, 583–591. [PubMed: 29713037]
30. Tanwar L; Börgel J; Ritter T Synthesis of Benzylic Alcohols by C—H Oxidation. J. Am. Chem. Soc 2019, 141, 17983–17988. [PubMed: 31689095]
31. Gomberg M An instance of Trivalent Carbon: Triphenylmethyl. J. Am. Chem. Soc 1900, 22, 757–771.
32. Jang ES; McMullin CL; Käß M; Meyer K; Cundari TR; Warren TH Copper(II) Anilides in sp^3 C—H Amination. J. Am. Chem. Soc 2014, 136, 10930–10940. [PubMed: 24940616]

33. Bower JK; Cypcar AD; Henriquez B; Stieber SCE; Zhang S C(sp^3)—H Fluorination with a Copper(II)/(III) Redox Couple. J. Am. Chem. Soc 2020, 142, 8514–8521. [PubMed: 32275410]
34. Kochi JK Electron-Transfer Mechanisms for Organometallic Intermediates in Catalytic Reactions. Acc. Chem. Res 1974, 7, 351–360.
35. Jenkins CL; Kochi JKI Ligand Transfer of Halides (Chloride, Bromide, Iodide) and Pseudohalides (Thiocyanate, Azide, Cyanide) from Copper(II) to Alkyl Radicals. J. Org. Chem 1971, 36, 3095–3102.
36. Jenkins CL; Kochi JK II. Kinetics of Ligand Transfer Oxidation of Alkyl Radicals. Evidence for Carbonium Ion Intermediates. J. Org. Chem 1971, 36, 3103–3111.
37. Jenkins CL; Kochi JK Homolytic and Ionic Mechanisms in the Ligand-Transfer Oxidation of Alkyl Radicals by Copper(II) Halides and Pseudohalides. J. Am. Chem. Soc 1972, 94, 856–865.
38. Kochi JK; Bemis A Carbonium Ions from Alkyl Radicals by Electron Transfer. J. Am. Chem. Soc 1968, 90, 4038–4051.
39. Kochi JK; Bemis A; Jenkins CL Mechanism of Electron Transfer Oxidation of Alkyl Radicals by Copper(II) Complexes. J. Am. Chem. Soc 1968, 90, 4616–4625.
40. Wayner DDM; McPhee DJ; Griller D Oxidation and Reduction Potentials of Transient Free Radicals. J. Am. Chem. Soc 1988, 110, 132–137.
41. Control experiments show that benzyl azides can racemize under the reaction conditions. See section 4 of the Supporting Information for details, in addition to the following reference: Ott AA; Topczewski JJ Catalytic Racemization of Activated Organic Azides Org. Lett 2018, 20, 7253–7256. [PubMed: 30394752]
42. Ellis GP; Lockhart IM; Meeder-Nycz D; Schweizer EE Chromenes, Chromanones, and Chromones In The Chemistry of Heterocyclic Compounds; Ellis GP, Ed.; John Wiley and Sons, Inc.: New York, 1977; Vol. 31, pp 1–1196.
43. Herzon SB; Woo CM The Diazofluorene Antitumor Antibiotics: Structural Elucidation, Biosynthetic, Synthetic, and Chemical Biological Studies. Nat. Prod. Rep 2012, 29, 87–118. [PubMed: 22037715]
44. Galiè N; Ghofrani HA; Torbicki A; Barst RJ; Rubin LJ; Badesch D; Fleming T; Parpia T; Burgess G; Branzi A; Grimminger F; Kurzyna M; Simonneau G Sildenafil Citrate Therapy for Pulmonary Arterial Hypertension. N. Engl. J. Med 2005, 353, 2148–2157. [PubMed: 16291984]
45. Hohnloser SH; Crijns HJGM; van Eickels M; Gaudin C; Page RL; Torp-Pedersen C; Connolly SJ Effect of Dronedarone on Cardiovascular Events in Atrial Fibrillation. N. Engl. J. Med 2009, 360, 668–678. [PubMed: 19213680]
46. Perkovic V; Jardine MJ; Neal B; Bompoint S; Heerspink HJL; Charytan DM; Edwards R; Agarwal R; Bakris G; Bull S; Cannon CP; Capuano G; Chu P-L; de Zeeuw D; Greene T; Levin A; Pollock C; Wheeler DC; Yavin Y; Zhang H; Zinman B; Meininger G; Brenner BM; Mahaffey KW Canagliflozin and Renal Outcomes in Type 2 Diabetes and Nephropathy. N. Engl. J. Med 2019, 380, 2295–2306. [PubMed: 30990260]
47. Rhodes JR Immunopotentiatory Agents and Physiologically Acceptable Salts Thereof. U.S. Patent 5508310A, 4 16, 1996.
48. Smith HW Cyclopentapyrazole and Tetrahydroindazole Compounds. Int. Patent. Appl WO8607357, 12 18, 1986.
49. Plosker GL Dapagliflozin: A Review of Its Use in Patients with Type 2 Diabetes. Drugs 2014, 74, 2191–2209. [PubMed: 25389049]
50. Peck AM; Kucklick JR; Schantz MM Synthetic Musk Fragrances in Environmental Standard Reference Materials. Anal. Bioanal. Chem 2007, 387, 2381–2388. [PubMed: 16906386]
51. LaRosa JC; Grundy SM; Waters DD; Shear C; Barter P; Fruchart J-C; Gotto AM; Greten H; Kastelein JJP; Shepherd J; Wenger NK Intensive Lipid Lowering with Atorvastatin in Patients with Stable Coronary Disease. N. Engl. J. Med 2005, 352, 1425–1435. [PubMed: 15755765]
52. Sajja Y; Vanguru S; Jilla L; Vulupala HR; Bantu R; Yogeswari P; Sriram D; Nagarapu L A Convenient Synthesis and Screening of Benzosuberone Bearing 1,2,3-Triazoles against Mycobacterium Tuberculosis. Bioorg. Med. Chem. Lett 2016, 26, 4292–4295. [PubMed: 27476139]

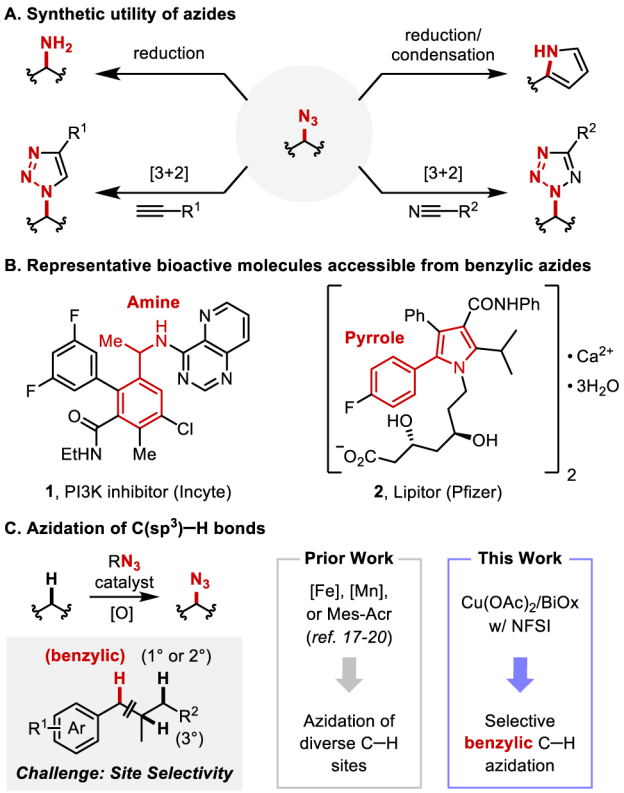

Figure 1.

Azides are important intermediates in organic syntheses (A) and medicinal chemistry (B) and are ideally prepared by direct azidation of sp^3 C—H bonds (C). NFSI, *N*-fluorobenzenesulfonimide. Mes-Acr, 9-mesityl-10-alkylacridinium catalyst.

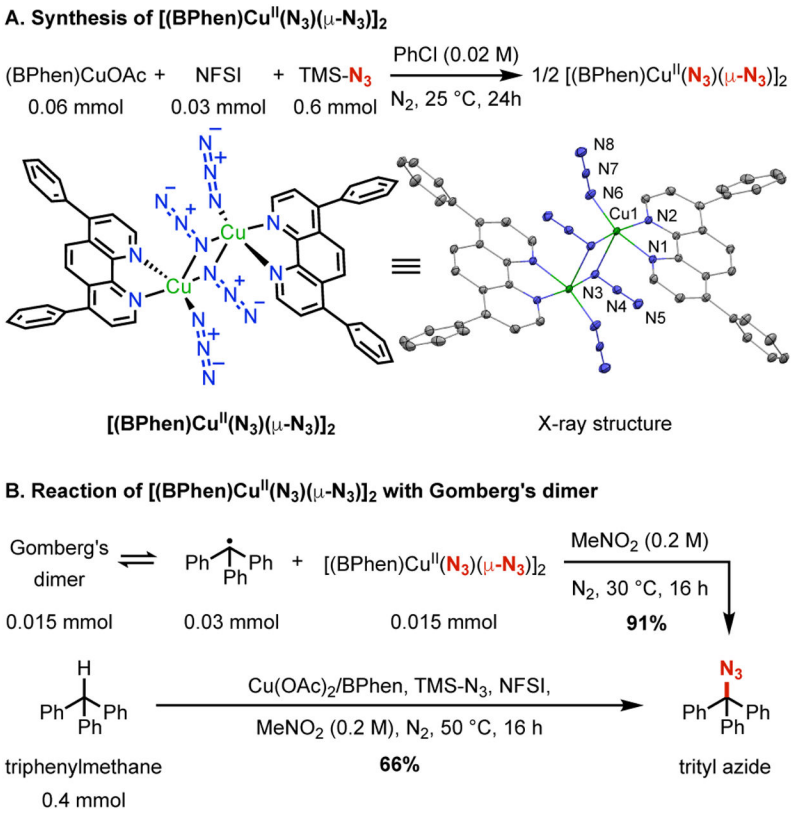

Figure 2.

(A) Synthesis and crystal structure of [(BPhen)Cu^{II}(N$_3$)(μ-N$_3$)]$_2$ (hydrogen atoms and chlorobenzene molecule omitted for clarity). (B) Reaction of [(BPhen)Cu^{II}(N$_3$)(μ-N$_3$)]$_2$ with Gomberg's dimer (6 mol% Cu(OAc)$_2$/BPhen, 3.6 equiv. TMSN$_3$, 2.5 equiv. NFSI).

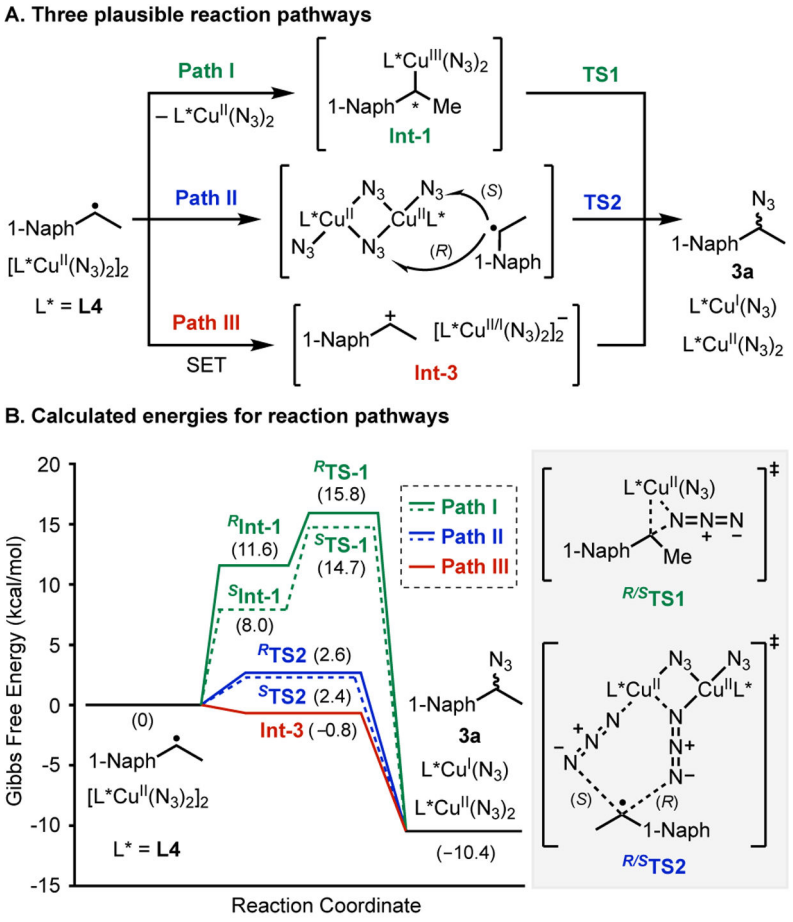

Figure 3.

Three proposed pathways for azidation of the benzyl radical (A), and simplified energy diagrams comparing the three pathways (B) (see text and Supporting Information for details).

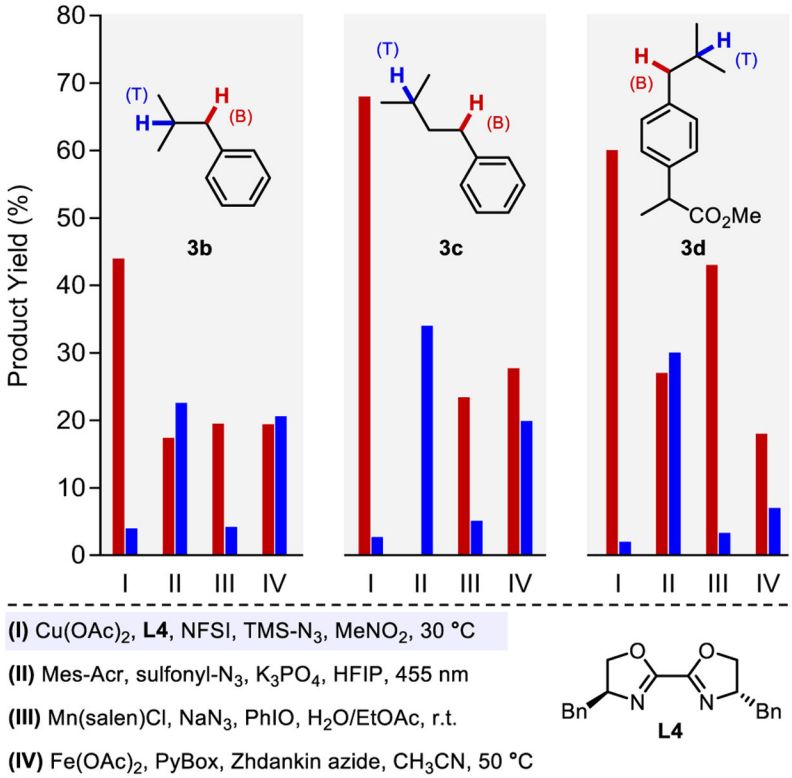

Figure 4.

Azidation site selectivity with different catalytic methods (see Section 5 in the Supporting Information for details). Standard condition for method I; substrate (0.4 mmol), $Cu(OAc)_2$ (2.0 mol%), BiOx (4.0 mol%), $TMSN_3$ (3.6 equiv.), NFSI (2.5 equiv.), 0.2 M $MeNO_2$, 30 °C, 24 h for **3b**, 48 h for **3c** and **3d**.

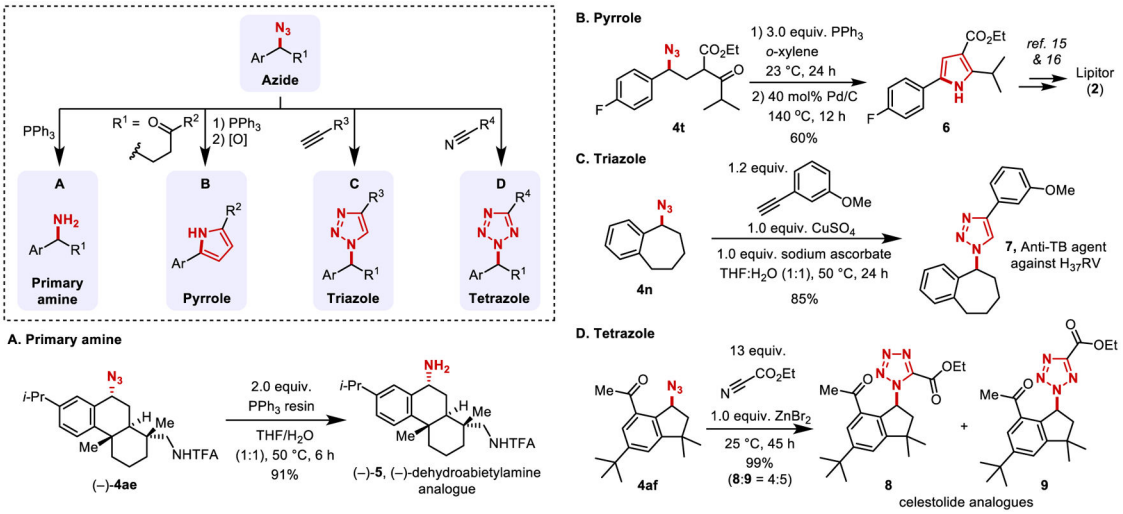

Figure 5.

Derivatization of azides to access primary amine in (−)-dehydroabietylamine (A), pyrrole in Lipitor precursor (B), triazole in anti-tuberculosis agent (C), and tetrazoles in celestolide analogues (D).

Table 1.

Reaction Optimization[a]

entry	catalyst (mol%), ligand (mol%)	NFSI (equiv.)	TMS-N_3 (equiv.)	Yield[b] (%)
1	CuOAc (10), **L1** (10) (room temp., solv = benzene)[22]	1.5	3.0	6
2	CuOAc (10), **L1** (10) (solv = benzene)	1.5	3.0	51
3	CuOAc (10), **L1** (10)	1.5	3.0	55
4	CuI (10), **L1** (10)	1.5	3.0	31
5	$Cu(acac)_2$ (10), **L1** (10)	1.5	3.0	42
6	$Cu(OAc)_2$ (10), **L1** (10)	1.5	3.0	62
7	$Cu(OAc)_2$ (10) (no ligand)	1.5	3.0	15
8	$Cu(OAc)_2$ (10), **L2** (10)	1.5	3.0	37
9	$Cu(OAc)_2$ (10), **L3** (10)	1.5	3.0	69
10	$Cu(OAc)_2$ (10), **L4** (10)	1.5	3.0	85
11	**$Cu(OAc)_2$ (2.0), L4 (4.0)**	**2.5**	**3.6**	**93**[c]

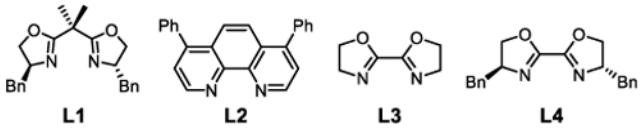

[a] 0.4 mmol **3a**.

[b] NMR yield, ext. std. = mesitylene.

[c] Isolated yield.

Table 2.

Scope of Alkylarene Benzylic C—H Azidation[a,b]

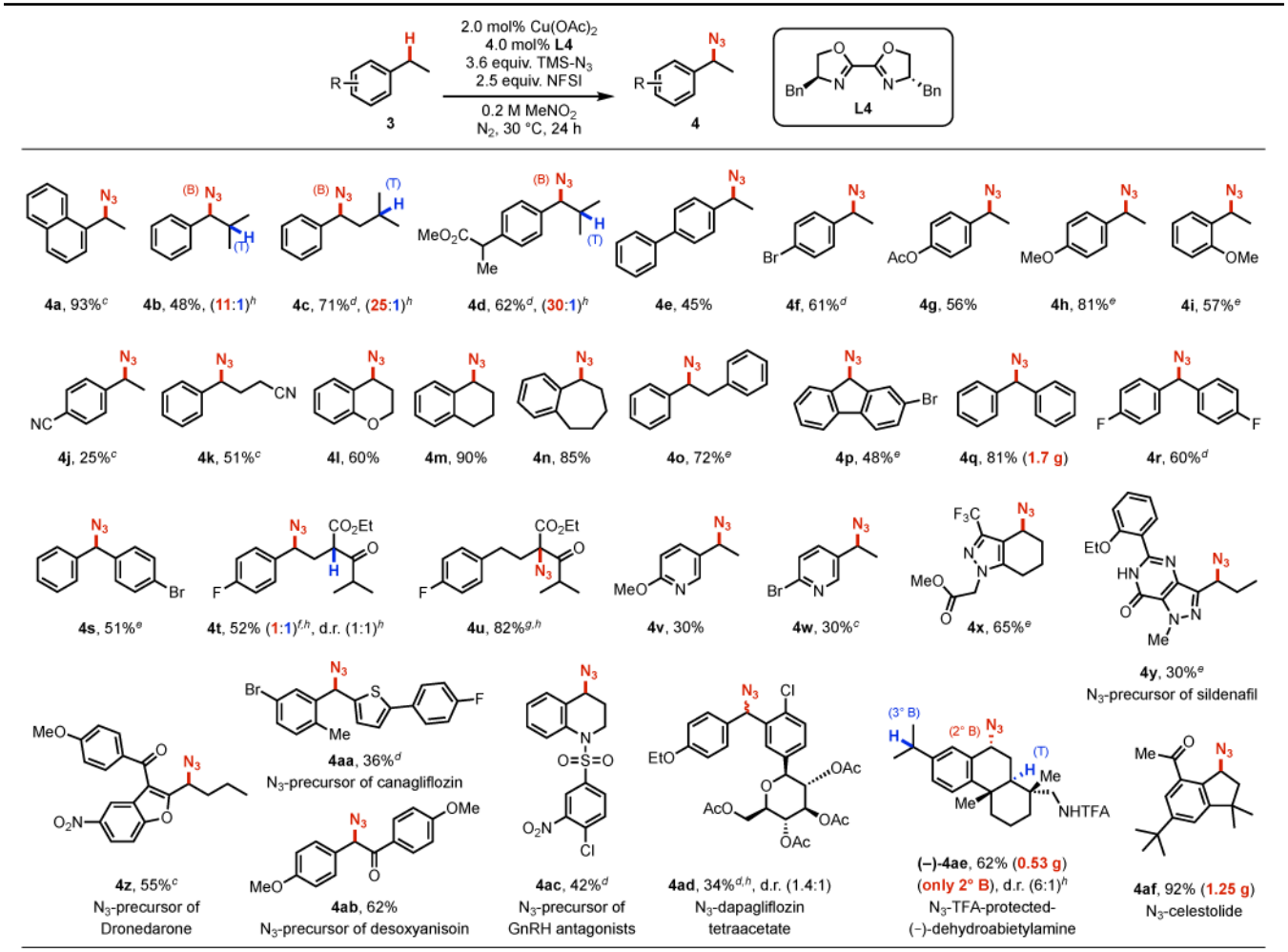

[a]Substrate (0.4 mmol).

[b] Isolated yield.

[c] Standard condition at 50 °C for 16 h.

[d] Standard condition for 48 h.

[e] Substrate (0.2 mmol), $Cu(OAc)_2$ (6.0 mol%), BiOx (12 mol%).

[f] Substrate (0.2 mmol), $Cu(OAc)_2$ (1.0 mol%), BiOx (2.0 mol%), 24 °C.

[g] 60 °C for 48 h.

[h] ^1H NMR analysis.